ARTICLE IN PRESS

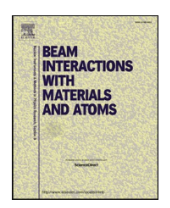
Nuclear Inst. and Methods in Physics Research B xxx (xxxx) xxx-xxx



Contents lists available at ScienceDirect

Nuclear Inst. and Methods in Physics Research B

journal homepage: www.elsevier.com/locate/nimb



Positive-ion accelerator mass spectrometry at ATLAS: Peaks and pits

Michael Paul^{a,*}, Richard C. Pardo^b, Philippe Collon^c, Walter Kutschera^d, K. Ernst Rehm^b, Robert Scott^b, Richard C. Vondrasek^b

- ^a The Hebrew University, Jerusalem 91904, Israel
- ^b Argonne National Laboratory, Argonne, IL 60439, USA
- ^c University of Notre Dame, Notre Dame, IN 46556, USA
- ^d University of Vienna, 1090 Vienna, Austria

ARTICLE INFO

Keywords: Accelerator mass spectroscopy ECR ion source Superconducting linear accelerator Gas-filled magnet Noble-gas radionuclides

ABSTRACT

Electron Cyclotron Resonance (ECR) ion sources and the production of multiple-charge positive ions with high efficiency in combination with a heavy-ion accelerator have opened the way to an alternative and complementary version of accelerator mass spectrometry (AMS). A notable strength of positive-ion over traditional AMS is the capability of ultra-high sensitivity detection of radioactive isotopes of noble gases, in particular 37 Ar ($t_{1/2} = 35$ d) and 39 Ar (269 y). The complete dissociation of molecular ions in the ECR and in particular of hydride ions of neighboring stable isotopes results in superior isotopic separation. However, the use of high charge states, necessary for acceleration to high energy, entails the existence of severe transmission degeneracies with stable ions having nearly equal mass-to-charge ratios, in addition to that of stable isobaric ions. Separation or discrimination of these parasitic ions require powerful and sophisticated dispersive systems at detection stage. We review here work performed and in progress at the ATLAS facility of Argonne National Laboratory (ANL) where an ECR ion source, a Radio-Frequency Quadrupole (RFQ), a superconducting linear accelerator and a Gas-Filled Magnet (GFM) are used as an AMS setup.

1. Introduction

Conventional accelerator mass spectrometry (AMS) has evolved based on electrostatic accelerators, mainly tandem accelerators and negative ion sources (see [1] for a recent review), this, in spite of the early works which utilized positive-ion cyclotrons. An article often cited as the first AMS experiment reported on the discovery of stable ³He at the Berkeley cyclotron [2]. Among the first AMS works of the modern era figures again the principle of radiocarbon (14C) dating with a positive-ion cyclotron [3] and so was later the first AMS detection of ⁴¹Ca [4,5]. The eventual dominance of negative-ion-based accelerator mass spectrometry is owed in part to the chemical selectivity of negative-ion formation (e.g. instability of the nitrogen negative ion in $^{14}\mathrm{C}$ detection) but also to the wide range of ions produced, especially from solid samples. This has however a significant limitation, namely the inapplicability to noble-gas radionuclides such as ³⁹Ar or ⁸¹Kr due to the instability of their negative ions and their inability to form abundant molecular ions. The use of electrostatic accelerators also sets a limit, depending on the accelerating voltage, to the mass range of analyzed nuclides, when isobaric discrimination is necessary.

The original thrust towards a positive-ion AMS capability at

Argonne National Laboratory was the development of an ultra-sensitive technique for the detection of cosmogenic 39 Ar ($t_{1/2} = 269$ y). The extremely low abundance of ³⁹Ar in the atmosphere (³⁹Ar/Ar = $(8.1 \pm 0.3) \times 10^{-16})$ was measurable in fact only in a laboratory specialized in low-level counting [6]. It was also clear for this case that isobaric separation of ubiquitous stable ³⁹K will require acceleration to high energy, which was in principle feasible using the Argonne Tandem Linear Accelerator System (ATLAS) [7] and the Electron Cyclotron Resonance (ECR) ion source [8]. The production of high ionic charge states by ECR ionization and acceleration to several MeV/u at ATLAS opened also the way to the detection of heavier rare radionuclides by AMS, not or hardly feasible with tandem accelerator mass spectrometry. Together with successes in this direction, a major drawback of the ECR ion source and utilization of high charge states proved to arise from contaminant beams of stable ion species (lighter or heavier and in addition to the isobaric species)) ionized by ECR so that their mass-tocharge (m/q) ratios are close to that of the rare ion to be detected which are then transported identically along the linear accelerator. Powerful separation and detection methods such as the Enge gas-filled magnetic (GFM) spectrograph or the Fragment Mass Analyzer (FMA) must be used in addition.

https://doi.org/10.1016/j.nimb.2019.04.003

Received 20 January 2018; Received in revised form 30 March 2019; Accepted 1 April 2019 0168-583X/ © 2019 Published by Elsevier B.V.

Please cite this article as: Michael Paul, et al., Nuclear Inst. and Methods in Physics Research B, https://doi.org/10.1016/j.nimb.2019.04.003

^{*} Corresponding author at: Racah Institute of Physics, Hebrew University, Jerusalem 91904, Israel. E-mail address: paul@vms.huji.ac.il (M. Paul).

M. Paul, et al.

In Section 2 of this paper, we present an overview of the ECR ion source and of the accelerator system at ATLAS, as used in AMS experiments. In Section 3, the setup used for 39 Ar AMS detection will be described. Recent AMS experiments involving 39 Ar and 37 Ar detection are presented and detection of 146 Sm with isobaric separation of the stable isotope 146 Nd, the heaviest to be successfully separated by AMS and the identification of rare actinides are reviewed in Section 4.

2. The ECR ion source

In a process curiously similar to that following the development of the negative-ion sputter source [9] for electrostatic tandem accelerators, the development of the Electron Cyclotron Resonance (ECR) ion source [10] provided a boost towards the production of high-energy heavy- (and light-) ions in positive-ion accelerators (cyclotrons and superconducting linacs) by allowing for the production of intense highly-charged ions. It is also interesting to note that in both cases the original development was essentially driven and accomplished by a single person, R. Middleton in the case of the high-intensity sputter negative-ion source [9] in the late 1970's and 80's and R. Geller in the 70's to 90's for the ECR ion source [10].

Fig. 1 shows a schematic diagram of the ECR ion source which consists of a plasma vacuum chamber fed with low-pressure gas (see below for solid samples) and microwave power. A specially designed configuration of multipolar magnetic field allows for the creation of a plasma confined within the chamber and of a resonance surface therein onto which the electron cyclotron resonance frequency

$$f_{ce}(GHz) = \frac{eB}{2\pi m_e} \sim 2.8B(kG) \tag{1}$$

is met. B is the magnetic field intensity and, $e,\ m_e$ are respectively the electron charge and mass. Electrons are accelerated to energies above the ionization potential of atoms and ions of the plasma successively ionized towards a distribution of charge states. A solenoidal magnetic field is superimposed at both ends of the chamber to contain longitudinally the plasma. The absence of resistively heated filaments or ionizers and the containment of the plasma within the chamber volume are among the main advantages of the ECR ion source over other types, contributing to its long lifetime, reliability and relative maintenance-free operation. The plasma critical parameters that control the performance of the ECR ion source are the electron temperature and density respectively determining the average electron accelerated energy and ion beam intensity and the ion confinement time allowing for charge breeding.

3. AMS with the ATLAS ECR ion source and accelerator

The ECR ion source and superconducting linear accelerator ATLAS

at Argonne National Laboratory allowed us to perform many AMS experiments, concentrating on those not feasible with conventional electrostatic tandem AMS facilities e.g. noble gas radionuclides, mediumheavy nuclides requiring isobaric discrimination. The two "classical pillars" of AMS, namely the ability to eliminate (or suppress sufficiently) the interference of stable molecular ion species and the discrimination power against isobaric nuclear species, are also here sustaining the technique. The former is achieved in conventional AMS based on electrostatic accelerators by stripping of fast ions (usually in the terminal of a tandem accelerator) passing through gas or a foil, which dissociates any molecular ion with a charge state q > 2. In the ECR ion source, molecular dissociation occurs within the plasma (see illustration in Fig. 2) through ionization by electrons accelerated to high kinetic energies on the ECR surface. Multiple ionization, depending on the ion confinement time in the plasma, leads to highlycharged ions which can be accelerated to high energy in a positive-ion accelerator, allowing thus for isobaric discrimination by nuclear detection methods as used in conventional AMS. The complete dissociation of molecular ions at the ECR ion stage leads to the elimination of the molecular fragments, in particular those of hydrides of neighboring stable isotopes, in the accelerated beam. Isotopic separation for medium and heavy nuclides is therefore superior to that of tandem AMS where fragments of negative hydride ions, dissociated by stripping in the highvoltage terminal produce background via charge-changing collisions in the residual gas.

Feeding the ECR ion source with the element (or enriched isotope) of interest is done either as a gas through a remotely-operated sapphire leak valve or from a solid sample, inserted into the plasma chamber via a radial port. A negative bias voltage applied to the sample holder results in sputtering by ions attracted from the plasma onto the material surface [11]. Resistively-heated ovens, often used as feeding mode in the ECR ion source, are not practical for AMS due to severe memory and cross-contamination effects. Highly-charged ions, extracted from the plasma chamber by an extraction voltage (around $15\,\mathrm{kV}$), proceed through a magnetic solenoid lens to a first (m/q) magnetic analysis and are then pre-accelerated from the ECR ion source platform to ground potential to an energy of $30\,\mathrm{keV}/u$ matching the Positive Ion Injector (PII) beam line.

The general layout of the ATLAS facility at Argonne National Laboratory is shown in Fig. 3, as used for most AMS experiments. The Positive Ion Injector (PII) beam line, originally composed of low- β superconducting resonators, includes presently as a first stage a (room-temperature) Radio-Frequency Quadrupole (RFQ) [12] accelerating and bunching ions (m/q < 7) from $30 \, \text{keV}/u$ to $296.5 \, \text{keV}/u$ into a continuous wave of micro-pulses at a frequency of $60.625 \, \text{MHz}$. The ions are then accelerated through a series of superconducting quarterwave and split-ring resonators, divided mainly for historical development reasons into a booster section and the ATLAS section and differing

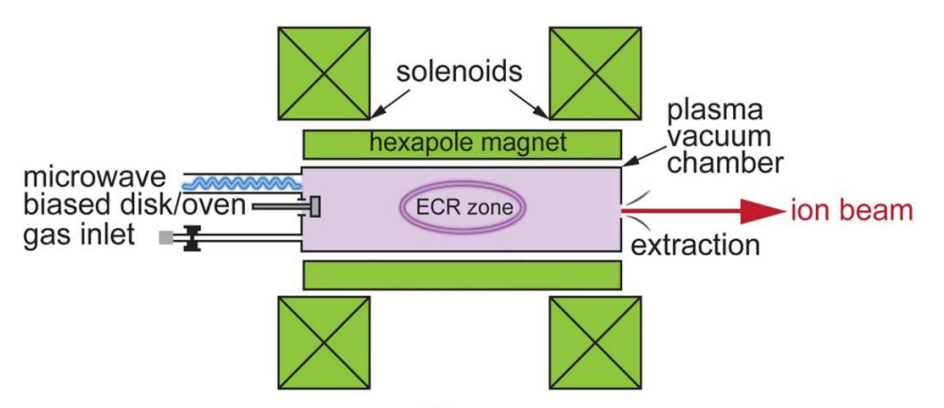


Fig. 1. Schematic diagram of the Electron Cyclotron Resonance ion source [10]; see text. The ellipse shown in the plasma chamber depicts the cross section of the surface onto which the electron cyclotron resonance (Eq. (1)) is met.

M. Paul, et al.

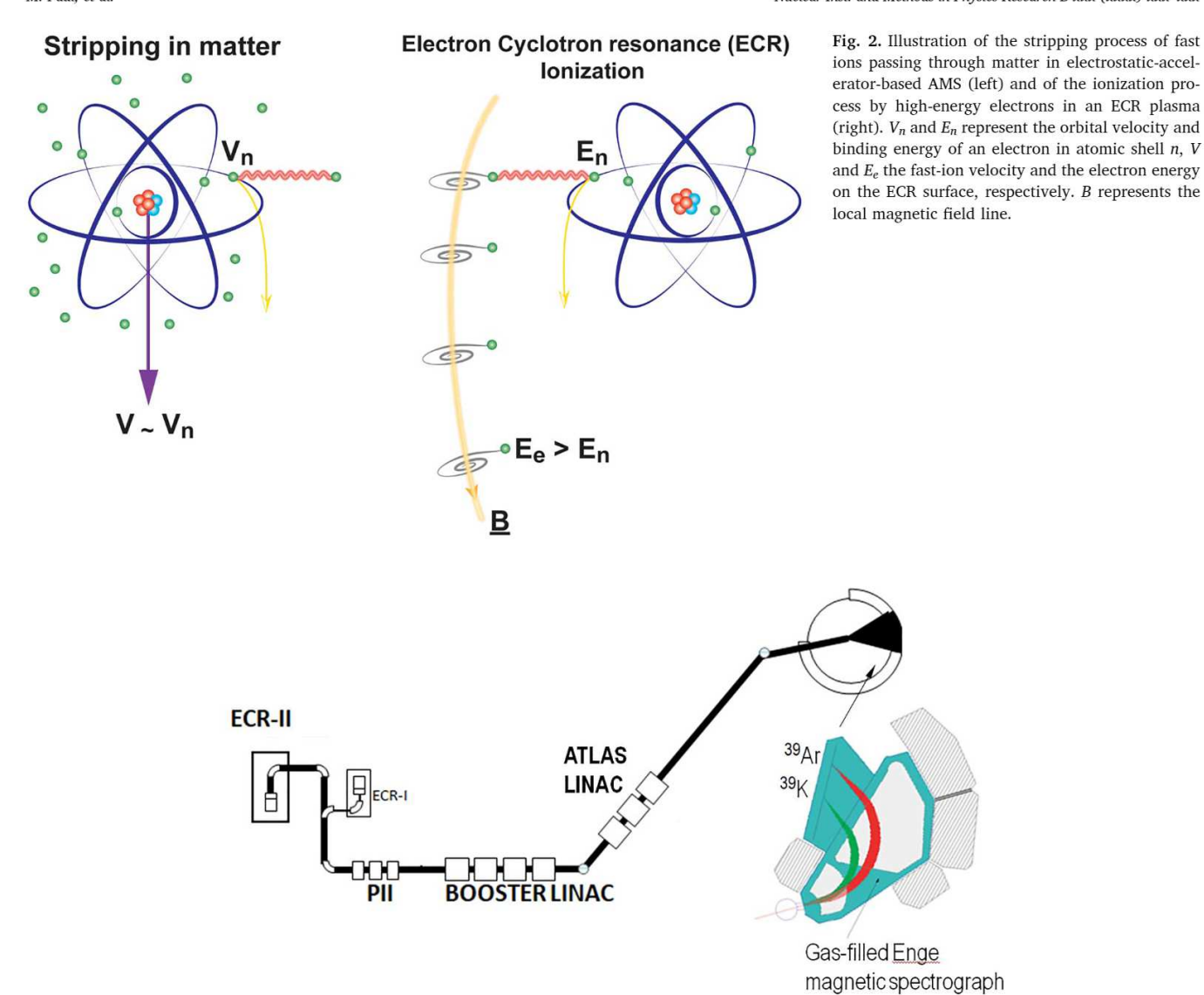


Fig. 3. General layout of the ATLAS facility as used for AMS experiments (left)and schematic diagram of the gas-filled Enge magnetic spectrograph (right). Isobaric separation of ³⁹Ar and stable ³⁹K (see text) in the focal plane of the gas filled spectrograph is depicted.

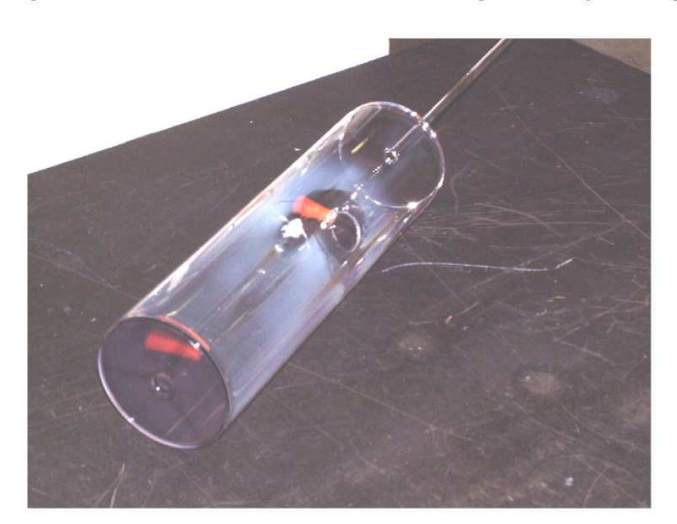


Fig. 4. Quartz liner inserted in the plasma vacuum chamber to reduce source background. The extraction orifice is seen on the lower left side while the hole on the cylindrical surface allows for radial insertion of the sputter sample.

in their optimal ion velocity matching. The final ion energy is massdependent and ranges from $\sim 15 \,\mathrm{MeV}/u$ for lighter (small m/q) ions down to $6-7 \,\mathrm{MeV}/u$ for heavier nuclei. Intermediate stripping is available between the two sections separated by a magnetic bend and is used in special cases for AMS. For a given final ion energy, every resonator along the structure is tuned to a given voltage amplitude and an independently determined phase, the latter defining a velocity profile along the accelerator which is specific to the mass-to-charge m/q ratio of the ion. This dependency on m/q allows us to tune the accelerator for the rare ion of interest by using a pilot beam of a stable ion having a nearly equal m/q (within a few percent, e.g. rare 39 Ar⁸⁺ vs stable ⁷⁸Kr¹⁶⁺) which can then be optimized by normal Faraday cups readings along the beam line. Final scaling correction of all ion-optical elements, determined by the precise m/q values of pilot and rare ions, is done for the rare ion. The procedure is analogous to that used in tandem AMS measurements when the rare ion is transported over the high-energy section at the same magnetic rigidity as a pilot beam (usually a stable isotope) by scaling appropriately the terminal accelerating voltage. In both cases, fractionation corrections apply usually, estimated by transporting different isotopic species. The property of the accelerator system to accelerate and transport identically ions having close-lying

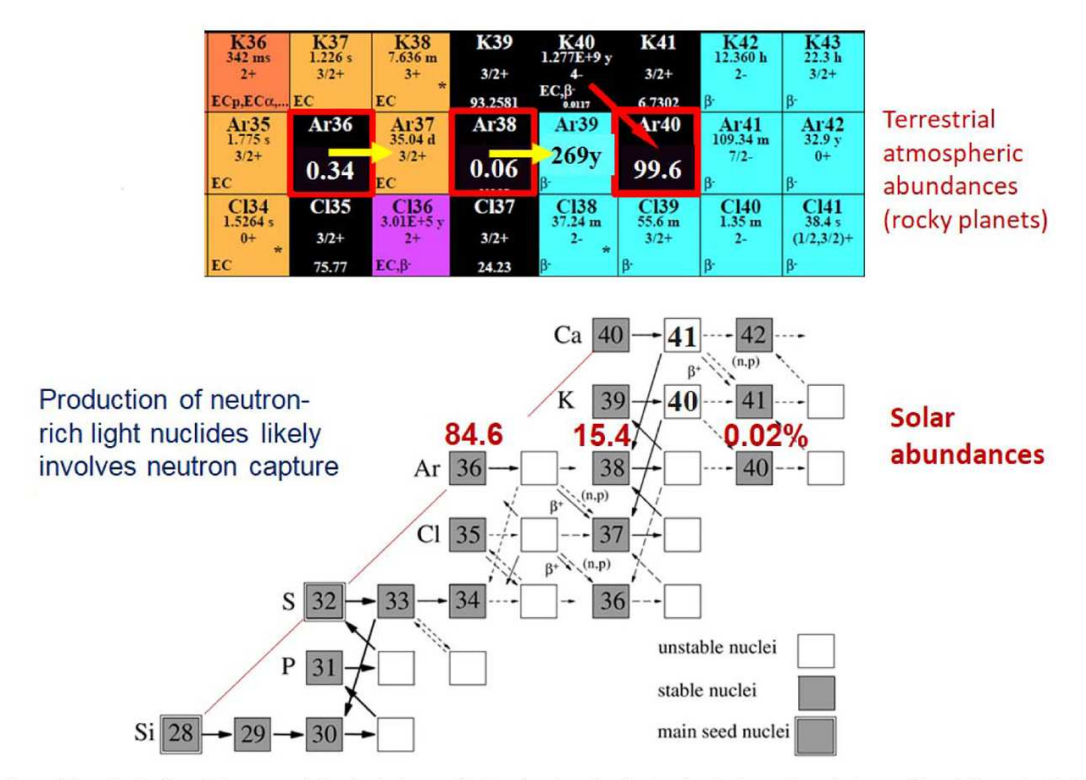


Fig. 5. (top) Portion of the chart of nuclides around the Ar isotopes; (bottom) network of astrophysical reactions between Si and Ca; note that the Ar isotopic abundances in the Solar system [22] are dominated by the lighter isotopes ³⁶Ar (along the alpha capture chain of explosive nucleosynthesis, red diagonal line) and ³⁸Ar. These are vastly different from the atmospheric terrestrial abundances listed in the chart of nuclides, dominated by radiogenic ⁴⁰Ar from ⁴⁰K decay [23]; the same is known to occur in other rocky planets e.g. Mars [24].

m/q values however results often in intense contaminant beams from sample chemical impurities and ion source structural material background. These contaminant ions need therefore to be separated or discriminated at the detection stage. The overwhelming intensity of such parasitic beams has sometimes led to the need of a liner, made of quartz, inserted inside the plasma chamber and covering most of the chamber walls, believed to be a source of this background (Fig. 4). Use of such a liner was shown to reduce the source background by a factor of up to 100 (see Section 4.2).

The detection system which has proved the most valuable so far in AMS experiments at the ATLAS facility is the gas-filled Enge magnetic spectrograph [13]. The gas-filled magnet disperses efficiently ions of different atomic numbers so that ions lighter or heavier than the rare ion to be detected are swept out of the focal plane detector (e.g. 78Kr16+ in the case of ³⁹Ar⁸⁺ detection) or blocked from entering the detector. Closer interferences, including the stable isobaric species (39K8+ vs ³⁹Ar⁸⁺) but sometimes other neighboring stable contaminant ions (e.g. $^{34}\mbox{S}^{7+},\,^{44}\mbox{Ca}^{9+},$ see Fig. 7) are present and need to be discriminated (see Section 4). Position measurement along the focal plane in a Parallel Grid Avalanche Counter (PGAC), time-of-flight (TOF) information between the fast anode signal of the PGAC and the RF master oscillator (which synchronizes the linac CW beam) and energy-loss signals in an ionization chamber mounted in telescope with the PGAC [14] provide identification spectra where the ion group of interest is isolated. Examples of selected cases are presented below in Section 4.

4. Positive-ion AMS experiments at ATLAS

A selection of positive-ion AMS experiments is presented below with the aim of emphasizing both the strengths and weaknesses of the technique.

4.1. Measurements of $^{36,38}Ar(n,\gamma)^{37,39}Ar$ neutron-capture cross sections

The neutron capture cross sections of the major argon Solar isotopes ^{36,38}Ar (see Fig. 5) are relevant to the nucleosynthesis of light nuclides on the neutron-rich side of the Z = N line. Cosmogenic production of ³⁷Ar (35 d) and ³⁹Ar (269 y), mainly due to neutron capture, makes these two nuclides interesting chronometers in the atmosphere and hydrosphere, respectively. The 36 Ar(n, γ) and 38 Ar(n, γ) thermal neutron capture cross sections were measured in 1950 [15] and 1952 [16], respectively; no previous experimental data exist for higher energy neutrons, relevant to stellar and atmospheric production. We describe here recent AMS experiments in which these cross sections were measured [17]. Irradiations of ³⁶Ar-enriched (99.935%) and ³⁸Ar (99.957%) gas, contained in 1 cm diameter Ti spherical shells (Fig. 6; [18]), were made with thermal neutrons from the Soreq IRR-1 nuclear reactor and with 45-keV quasi-Maxwellian neutrons. The latter were produced by the Li(p,n) reaction at the SARAF-LiLiT facility [19,20,21] with an intense proton beam impinging on the liquid-lithium target LiLiT (Fig. 6).

The AMS detection of 39 Ar using the setup described in Section 3 has been previously shown [25] to reach the ultra-high sensitivity needed for detection of cosmogenic 39 Ar (atmospheric concentration: $(8.1 \pm 0.3) \times 10^{-16}$ [26]). The isotopic ratios produced by neutron irradiation for cross section determination are much higher $(10^{-11}$ – $10^{-13})$ making the need for high beam currents (required for measurements of natural 39 Ar/Ar ratios) much less stringent. Consequently, the ECR ion source could be operated (without quartz liner) at low microwave power (60 W) and thus reduce interference of plasma

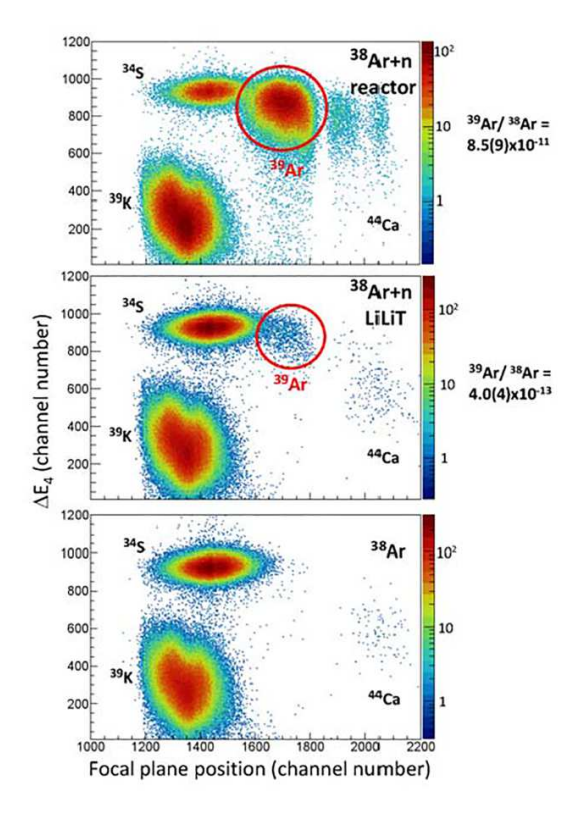


Fig. 6. (clockwise from top left) titanium sphere filled with isotopically enriched Ar (\sim 25 bars); schematic diagram of the Liquid-Lithium Target (LiLiT): the proton beam (\sim 3 kW) impinges (windowless) on a liquid-lithium film flowing in vacuum at a velocity of \sim 2.5 m/s to dissipate the beam power by transport. Neutrons with a quasi-Maxwellian energy distribution are produced at forward angles and irradiate the gas sphere; the gas-filled activated sphere mounted on a custom-made valve tool [18]; sphere and valve tool are installed on the ECR ion source port via a remote-controlled sapphire leak valve.

ions with the chamber walls, believed to be a source of background beam contaminants and resulting in a relatively low $^{39}\mathrm{K}$ isobaric count rate (see below). $^{39}\mathrm{Ar^{8+}}$ and $^{38}\mathrm{Ar^{8+}}$ ions extracted from the ECR ion source were alternately accelerated to 6 MeV/u by scaling the accelerator tuning parameters according to the m/q ratio of the two ions. The beam transmission from the PII entrance (see Fig. 3) to the last Faraday cup before detection was around 40% and was found consistent for $^{38}\mathrm{Ar}$ and $^{40}\mathrm{Ar}$ ions, therefore requiring no correction for the determination of the $^{39}\mathrm{Ar}/^{38}\mathrm{Ar}$ ratio. The validity of this determination is confirmed by the good agreement obtained for our measured $^{38}\mathrm{Ar}(n,\gamma)^{39}\mathrm{Ar}$ cross section [17] at thermal energy with its previous determination [16]. $^{39}\mathrm{Ar}$ ions were counted in the focal plane detector of the Enge gas-filled

spectrograph (Fig. 3) after proper identification and software gating (Fig. 7), using the different detector signals. The charge current of $^{38}\mathrm{Ar^{8+}}$ ions is measured in a suppressed Faraday cup, located just before the Enge spectrograph entrance. An identification spectrum of $^{39}\mathrm{Ar}$ ions and $^{39}\mathrm{Ar/^{38}Ar}$ ratios measured in repeated runs are shown in Fig. 7. The $^{38}\mathrm{Ar}$ (n, γ) $^{39}\mathrm{Ar}$ cross section σ_{39} is extracted from the measured $r_{39} = ^{39}\mathrm{Ar/^{38}Ar}$ isotopic ratio and the neutron fluence ϕt monitored during irradiation by the relation $\sigma_{39} = r_{39}/\phi t$. The cross section data from this experiment and their astrophysical significance were published posteriorly to this Conference [17].

The 36 Ar-filled spheres were irradiated similarly as described before and detection of the 37 Ar radionuclide by AMS was achieved for the first



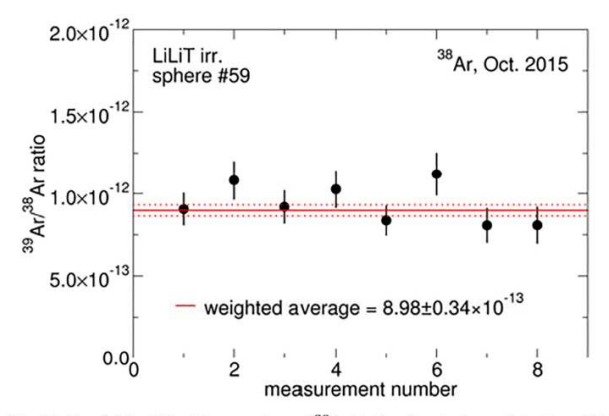


Fig. 7. (top) Identification spectra of ³⁹Ar in the focal-plane detector of the gasfilled Enge spectrograph. The horizontal axis represents the distance along focal plane and the vertical the energy loss signal in the last anode of the ionization detector. The ³⁹Ar group is well separated from the stable ³⁹K isobar. The ³⁴S ions, from source background, are transported as ³⁴S⁷⁺ ions, nearly degenerate in m/q with ³⁹Ar⁸⁺ ions; (bottom) Repeated measurements of the ³⁹Ar/³⁸Ar ratio.

time in these experiments. 37 Ar, decaying by pure electron capture (no γ emitted) with a half-life of 35.0 days, is notable for its role in R. Davis' experiment [27] in which its detection by Auger electron counting served as a measure of the Solar neutrino flux via the inverse β - decay reaction 37 Cl(ν , e⁻) 37 Ar. Low-level counting (LLC) of 37 Ar cosmogenic activity was also developed by Loosli, Oeschger and Wiest [28] and Riedmann and Purtschert [29] for tracer studies in the atmosphere and in water reservoirs and environmental monitoring. In our experiments,

it was decided to cross-calibrate 37Ar detection by AMS with LLC on the same irradiated samples to benchmark the absolute isotopic ratios measured in the AMS experiments. ³⁷Ar⁸⁺ ions, similarly produced as for ³⁹Ar detection, were accelerated through the ATLAS linac but the isobaric 37Cl background proved too intense to be accepted at the detection stage. The ${}^{37}\text{Ar}^{8+}$ ions were then stripped at 5.7 MeV/u between two stages of the linac (Fig. 8) and fully stripped 37Ar18+, discriminating from 37 Cl (Z = 17), were transported to the detection system. The detection system in this case consisted of a telescope of Si detectors, 50 µm and 300 µm thick. Spectra accumulated for the $^{37}\text{Ar}^{8+}$ - $> ^{37}\text{Ar}^{18+}$ tuning were clean of any background (Fig. 9). However, the stripping process introduced in this case an isotopic fractionation which was estimated by interpolating between the transmission of stable ³⁶Ar¹⁸⁺ and ³⁸Ar¹⁸⁺ beams; the transmission for the fully-stripped ${}^{37}Ar^{8+} - > {}^{37}Ar^{18+}$ beam was determined as 1.84(18)%. It is to be noted that this effective fractionation is not inherent to the stripping probability which is expected to be identical for ^{36,37,38}Ar ions, having the same velocity profile along the accelerator; the fractionation is attributed to the sensitive dependence of the transmission on ion-optical tuning of elements following the stripping. Spectra accumulated for the LiLiT-irradiated ³⁶Ar gas sample and for a non-irradiated $^{36}\mathrm{Ar}$ gas sample were background-free and are shown in Fig. 9. One ³⁷Ar count detected for the latter sample over 6.5 h, likely due to a memory effect in the ion source, corresponds to a concentration 37 Ar/ 36 Ar = 9×10^{-16} .

Fig. 10 shows the excellent agreement between the 37 Ar/ 36 Ar ratios measured by AMS and LLC [30] on aliquots of the same three samples, irradiated by quasi-Maxwellian ($kT \sim 45$ -keV) neutrons from LiLiT, epithermal (Cd-shield) and thermal + epithermal neutrons. The two latter irradiations were performed in the rabbit pneumatic transfer setup of the Soreg IRR1 nuclear reactor. The LLC measurements were made at University of Bern by counting Auger electrons in an underground internal ionization counter facility [29,30]. The sensitivity of AMS $(^{37}Ar)^{36}Ar \sim 1 \times 10^{-15}$), demonstrated by the present blank measurement was achieved with a low-intensity $^{36}\mathrm{Ar}^{8+}$ beam current. Extrapolating this sensitivity to an Ar current of 10 uA (readily achievable, see [25]), would correspond in the same conditions to a ³⁷Ar specific activity of 6 mBq/m³(air). It is interesting to compare this sensitivity to the Minimum Detectable Activity (MDA) of LLC which is in the range 0.6–29.0 mBq/m³(air) [29], limited by ³⁹Ar background. It seems thus that AMS may provide a complementary detection method for some environmental samples since the ³⁷Ar detection by AMS is independent of 39Ar background.

4.2. Isobaric separation in medium-mass nuclides

As mentioned in the introduction, highly-charged positive ions can be accelerated in the linear accelerator at ATLAS to energies high enough for isobaric discrimination up to medium-mass nuclides. We reproduce as an example the identification spectra of the alpha-decaying nuclide 146Sm, separated from the stable isobar 146Nd in the gas-filled magnetic spectrograph (Fig. 11) when accelerated to 6 MeV/u at ATLAS [31]. The use of a quartz liner (Fig. 4) in the ECR ion source was necessary in these measurements. We refer to [31] for details of the measurement technique in this case and especially for the absolute determination of the ¹⁴⁶Sm/¹⁴⁷Sm isotopic ratio performed by measuring the count rates of both ¹⁴⁶Sm and ¹⁴⁷Sm in the GFM detector, the latter being quantitatively attenuated. The AMS measurements of the $^{146}\mathrm{Sm}/^{147}\mathrm{Sm}$ isotopic ratios combined with the ratio of the alpha activities A_{146}/A_{147} in the same samples and the precisely known $^{147}\mbox{Sm}$ half-life (107.0(9) Gy [32]) enabled the determination of a new value for the 146Sm half-life (68(7) My [31]), 34% smaller than the adopted

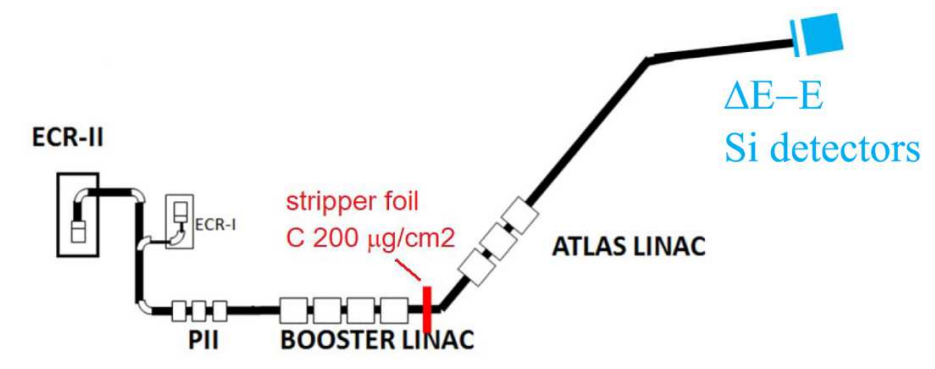


Fig. 8. Setup for AMS detection of 37 Ar detection at ATLAS: 37 Ar $^{8+}$ ions are fully stripped to 37 Ar $^{18+}$ between two acceleration stages and transported via magnetic analysis to a Δ E-E telescope of Si detectors. The full stripping and magnetic analysis totally eliminates the 37 Cl isobaric and other background ions.

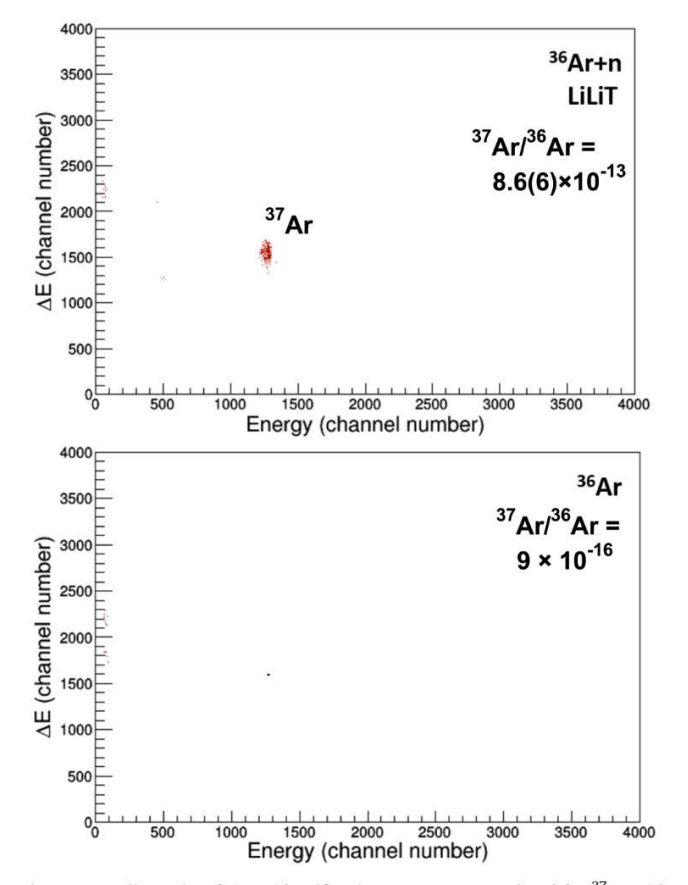


Fig. 9. Two-dimensional ΔE -E identification spectra accumulated for ³⁷Ar with the setup illustrated in Fig. 8 for the LiLiT-irradiated ³⁶Ar (top) and for the non-irradiated ³⁶Ar (bottom) sample (see text).

value of 103(5) My [33]. The main geo/cosmochemical application of ¹⁴⁶Sm is dating of planetary processes that occurred early in the history of the Solar system. The abundance of the ¹⁴⁶Sm decay product, ¹⁴²Nd, in some early solar system lunar samples (measured as the isotopic ratio ¹⁴²Nd/¹⁴⁴Nd) is better explained with the new (68 My) half-life [31,34]. At the same time, the previous value (103 My) of the ¹⁴⁶Sm half-life fits better other lunar and meteorite samples [35]. We consider the value of the ¹⁴⁶Sm half-life as still uncertain and more measurements are needed in order to determine it accurately.

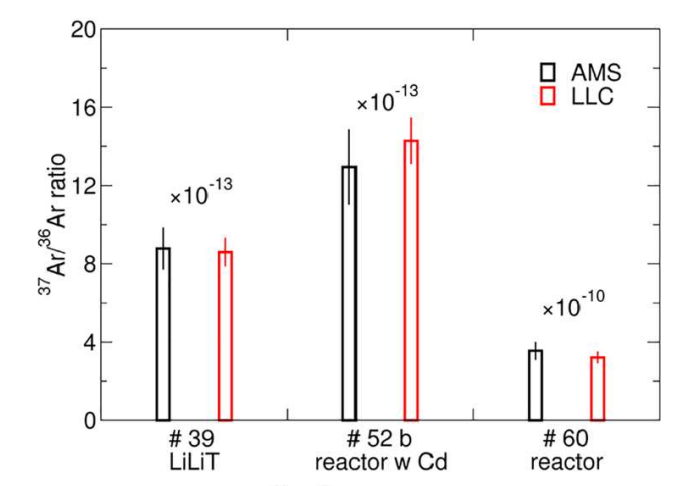


Fig. 10. Comparison between 37 Ar/ 36 Ar ratios measured in aliquots of the same irradiated gas samples by AMS and LLC (U. of Bern) (see text). Uncertainties are shown as vertical bars.

4.3. Detection of actinides with positive-ion AMS

We review here for completeness the use of positive-ion AMS at ATLAS for ultra-sensitive mass spectrometry of actinides [36]. We refer also to R. Pardo et al. [37] in these Proceedings for a recent use of the method to the measurement of neutron and multiple-neutron capture cross section of rare actinides. The essential feature of the method in this case is the elimination of molecular ions by the ECR ionization process and subsequent m/q analysis in the acceleration and transport system. In the experiment reported in [36], natural U ore samples were prepared as pressed U₃O₈ + C cathodes and the ECR source was operated in the sputtering mode (Section 3). ²³⁶U²¹⁺ ions were selected from the source and accelerated in ATLAS to 221 MeV without further stripping. A beam of 124Xe11+ served as pilot beam. Due to the high magnetic rigidity of the U ions above the range of the Enge magnetic spectrograph, analysis and detection of U ions were done in this case with the Fragment Mass Analyzer (FMA). Stripping was required to reduce the beam rigidity to the acceptance limits of the FMA elements; the ions were stripped in a 60 μg/cm² C target in front of the FMA. The $^{236}\mathrm{U}^{39+}$ ions were analyzed in the FMA by m/q via a succession of magnetic and electrostatic deflection and eventually detected along the focal plane in a position-sensitive PGAC detector followed by a Si detector. An overall abundance sensitivity (ratio of the abundances of separated neighboring isotopes) of 1×10^{-14} was established in the experiment. Fig. 12 [36] shows the identification of ²³⁶U (23.4 My) in a

M. Paul. et al.

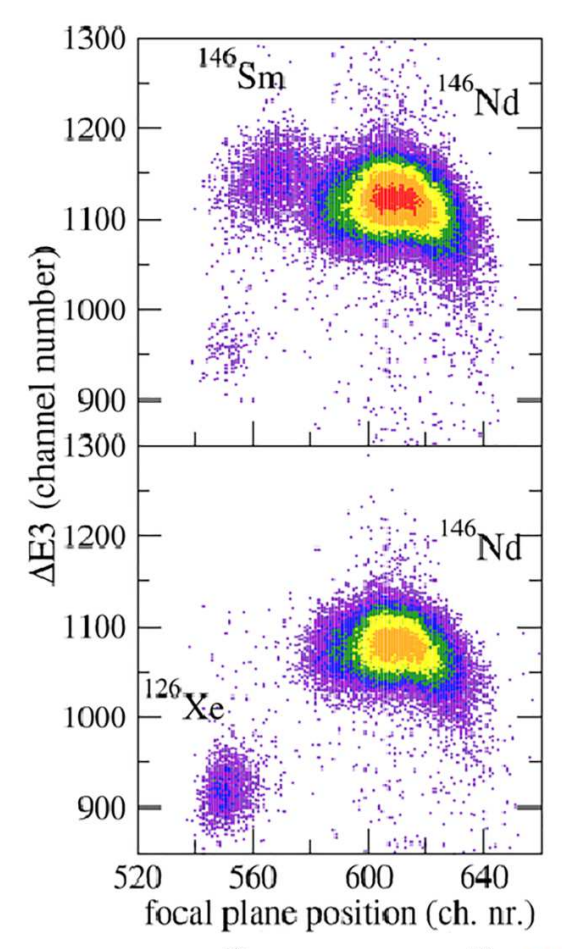


Fig. 11. Isobaric separation of ¹⁴⁶Sm from its stable isobar, ¹⁴⁶Nd [31] at an energy of 6 MeV/u in the focal plane of the gas-filled Enge magnetic spectrograph (horizontal axis). The vertical axis is the energy-loss signal measured in the third anode of the ionization detector. The upper spectrum is measured for a ¹⁴⁷Sm sample irradiated with fast neutrons, where ¹⁴⁶Sm is produced by the $^{147}\mathrm{Sm}(\mathrm{n,2n})^{146}\mathrm{Sm}$ reaction, the lower spectrum is measured for a high-purity natural Sm sample, establishing a sensitivity limit 146 Sm/ 147 Sm $\sim 10^{-11}$

natural pitchblende Joachimstahl mineral with a concentration $^{236}\mathrm{U}/$ $U = 1.1 \times 10^{-10}$ [38]. Fig. 12 illustrates the severe problem caused in ECR-AMS by ions with near m/q degeneracy originating from source (and sample) background.

5. Conclusion

We have reviewed the potential of the positive-ion AMS technique using highly-charged ions created in an ECR ion source followed by acceleration in the ATLAS superconducting linear accelerator. The experiments described emphasize the peculiarity of this type of accelerator mass spectrometry: ultra-sensitive detection of noble-gas radionuclides, detection and isobaric separation for medium-heavy radionuclides. The major drawback of the technique is the high sensitivity to parasitic ions due to source material and/or to sample chemical impurities transported to the detection system when their charge-tomass ratio is close to that of the measured ion. It can be expected that new linac machines that can deliver high intensity and high quality heavy ion beams, together with sophisticated ion analysis and detection instruments, may expand the sensitivity and range of detection of rare ions, especially so in the higher mass region still largely unexplored.

This research is based upon work supported by the U.S. Department of Energy, Office of Science, Office of Nuclear Physics, under contract number DE-AC02-06CH11357. This research used resources of ANL's

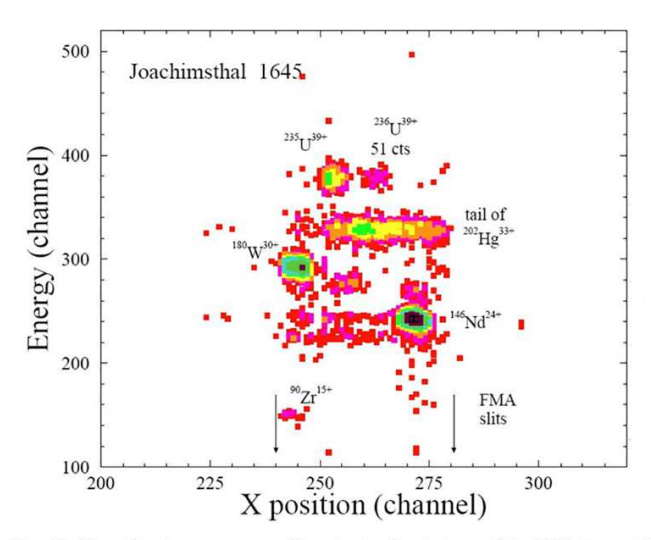


Fig. 12. Identification spectrum of ions in the focal plane of the FMA. Ions with different m/q values are dispersed along the horizontal axis; the vertical axis represents the ion energy measured in a Si detector. Slits in front of the focal plane around the region of interest are set to reduce count rate from background ions in the detector. After stripping in front of the FMA, 236U39+ ions $(^{236}\text{U/U} = 1 \times 10^{-10})$ are separated from ^{235}U and from background ions transported along the ATLAS accelerator due to a m/q near-degeneracy with the accelerated 236U21+ ions.

ATLAS facility, which is a DOE Office of Science User Facility. M.P. gratefully acknowledges support of the Pazy Foundation (Israel) and Israel Science Foundation (Grant 1387/15).

References

- [1] W. Kutschera, Adv. Phys. X 1 (4) (2016) 570.
- [2] L.W. Alvarez, R. Cornog, Phys. Rev. 56 (1939) 379.[3] R.A. Muller, Science 196 (1977) 489.
- [4] G.M. Raisbeck, F. Yiou, Symp. on Accelerator Mass Spectrometry, Argonne National Laboratory, ANL/PHY-81-1, 1981, p. 23.
- [5] G. Raisbeck, F. Yiou, Nature 277 (1979) 42.
- [6] H.H. Loosli, et al., Nucl. Instr. Meth. Phys. Res. B 17 (1986) 402.
- L.M. Bollinger, IEEE Trans. Nucl. Sci. NS-30 (4) (1983) 2065.
- R.C. Pardo, P.J. Billquist, Rev. Sci. Instrum. 61 (1990) 239. R. Middleton, Nucl. Instr. Meth. In Phys. Res. A 214 (1983) 139.
- [10] R. Geller, Electron Cyclotron Resonance Ion Sources and ECR Plasmas, IOP, Bristol and Philadelphia, 1996.
- [11] R. Harkewicz, P.J. Billquist, J.P. Greene, J.A. Nolen, R.C. Pardo, Rev. Sci. Instr. 66 (1995) 2883
- [12] P.N. Ostroumov, et al., Phys. Rev. ST Accel. Beams 15 (2012) 110101.
- M. Paul, et al., Nucl. Instr. Methods A277 (1989) 418.
- [14] M. Paul, et al., ANL Rep. 97 (14) (1996) 79.
- [15] G.E. McMurtrie, D.P. Crawford, Phys. Rev. 77 (1950) 840.
- S. Katcoff, Phys. Rev. 87 (1952) 886.
- M. Tessler, et al., Phys. Rev. Lett. 121 (2018) 112701.
- [18] G. Rupp, et al., Nucl. Instr. Meth. Phys. Res. A 608 (2009) 152. S. Halfon, et al., Rev. Sci. Instr. 84 (2013) 12350.
- S. Halfon, et al., Rev. Sci. Instr. 85 (2014) 056105.
- [21] M. Tessler, et al., Phys. Lett. B 751 (2015) 418.
- K. Lodders, Astrophys. J. 591 (2003) 1220.
- [23] C.F. von Weizsaecker, Physik. Z. 38 (1937) 623.
- E. Anders, T. Owen, Science 198 (1977) 453.
- Ph. Collon, et al., Nucl. Instr. Meth. Phys. Res. B 223-224 (2004) 428.
- [26] H.H. Loosli, Earth Planet. Sci. Lett. 63 (1983) 51.
- R. Davis, Prog. Part. Nucl. Phys. 32 (1994) 13.
- H.H. Loosli, H. Oeschger, W. Wiest, J. Geophys. Res. 75 (1970) 2895.
- R. Riedmann, R. Purtschert, Environ. Sci. Technol. 45 (2011) 8656.
- Measurements done by R. Purtschert, U. of Bern, (2017).
- N. Kinoshita, et al., Science 335 (2012) 1614.
- K. Kossert, et al., Appl. Radiat. Isot. 67 (2009) 1702.
- F. Meissner, W.-D. Schmidt-Ott, L. Ziegeler, Z. Phys, A 327 (1987) 171.
- [34] M. Gaffney, L.E. Borg, Geochimica et Cosmochimica Acta 140 (2014) 227.
- N.E. Marks, et al., Earth Planet. Sci. Lett. 405 (2014) 15
- [36] M. Paul, Nucl. Instr. and,, et al., Methods in Phys, Res. B 172 (2000) 688.
- [37] R. Pardo et al., These Proceedings.
- [38] D. Berkovits, et al., Nucl. Instr. Methods in Phys Res. B 172 (2000) 372.